

Effect of groundwater level change on piled raft foundation in Ho Chi Minh City, Viet Nam using 3D-FEM

Kamol Amornfa*¹, Ha T. Quang^{1a} and Tran V. Tuan^{2b}

¹Department of Civil Engineering, Faculty of Engineering at Kamphaeng Saen, Kasetsart University, Kamphaeng Saen, Nakhon Pathom, Thailand

²Department of Civil Engineering, College of Engineering Technology, Can Tho University, Ninh Kieu, Can Tho, Viet Nam

(Received July 12, 2022, Revised January 15, 2023, Accepted January 18, 2023)

Abstract. Ground subsidence, which is a current concern that affects piled raft foundations, has occurred at a high rate in Ho Chi Minh City, Viet Nam, due primarily to groundwater pumping for water supply. In this study, the groundwater level (GWL) change affect on a piled raft foundation was investigated based on the three-dimensional finite element method (3D-FEM) using the PLAXIS 3D software. The GWL change due to global groundwater pumping and dewatering were simulated in PLAXIS 3D based on the GWL reduction and consolidation. Settlement and the pile axial force of the piled raft foundation in Ho Chi Minh subsoil were investigated based on the actual design and the proposed optimal case. The actual design used the piled foundation concept, while the optimal case applied a pile spacing of 6D using a piled raft concept to reduce the number of piles, with little increased settlement. The results indicated that the settlement increased with the GWL reduction, caused by groundwater pumping and dewatering. The subsidence started to affect the piled raft foundation 2.5 years after construction for the actual design and after 3.4 years for the optimal case due to global groundwater pumping. The pile's axial force, which was affected by negative skin friction, increased during that time.

Keywords: 3D-FEM; axial load; ground subsidence; groundwater level; Ho Chi Minh subsoil; piled rafts; settlement

1. Introduction

Piled raft foundations are widely used worldwide (Bernardes *et al.* 2019, Huang *et al.* 2017, Katzenbach *et al.* 2000, Poulos 2012, Tan *et al.* 2006, Yamashita *et al.* 2015, Yamashita *et al.* 2011) as effective foundation method for high-rise buildings in soft clay subsoil (Amornfa *et al.* 2012, Khanmohammadi and Fakharian 2018, Kitiyodom *et al.* 2011, Quang *et al.* 2021, Watcharasawe *et al.* 2021). The combined piles and raft can reduce the number of piles compared to the concept of a piled foundation because a part of the applied load transfers directly to the soil beneath the raft (Bandyopadhyay *et al.* 2020, Katzenbach *et al.* 2000, Nakanishi and Takewaki 2013, Sawada and Takemura 2014). However, there are many problems, such as bearing capacity, settlement, and the load share between piles and raft as effect the piled raft foundation (Fattah *et al.* 2013, Gu *et al.* 2016, Hoang and Matsumoto 2020, Ko *et al.* 2018). In particular, a current concern is subsidence due to the groundwater affecting the piled raft foundation (Vali and Foroughi Boroujeni 2022, Vali *et al.* 2017).

The GWL should be considered in the foundation

design, as depending on the GWL, the effective stress will change. Thus, the behavior of the foundation will change due to changes in the GWL.

In Ho Chi Minh City, Viet Nam, groundwater has been used as a water source since 1920. In 1990, the country's economic policies changed, resulting in increased demand for groundwater. Nowadays, industrialization and urbanization have driven the rapid increase in the number of groundwater pumps; however, no charges and policies to control groundwater pumping were applied (Vo 2008) so that ground subsidence, affecting the infrastructure in general and the foundation of building in particular, has occurred frequently and is increasing annually due to the groundwater pumping (Minh *et al.* 2015, Thoang and Giao 2015). Furthermore, building works can have an impact on the foundation of adjacent buildings. Groundwater pumping, also known as dewatering, is commonly used in excavation, foundation construction, and basement floor construction.

Tran *et al.* (2012) investigated, the effect of GWL change on piled raft foundation, based on drained and undrained conditions. They reported that the settlement of the foundation and the axial force increased as the GWL decreased. The axial load capacity was the most significant change due to the GWL change (Roh *et al.* 2019). The behavior of piled raft foundation due to GWL change was evaluated based on the 3D-FEM using the PLAXIS 3D software (Beygi *et al.* 2019).

In this paper, the effect of ground subsidence due to reducing global groundwater pumping and dewatering on the piled raft foundation in Ho Chi Minh City was studied based on 3D-FEM and the PLAXIS 3D program.

*Corresponding author, Assistant Professor

E-mail: fengkma@ku.ac.th

^aMaster student

E-mail: hatran.q@ku.th

^bDoctor

E-mail: tvtuan@ctu.edu.vn

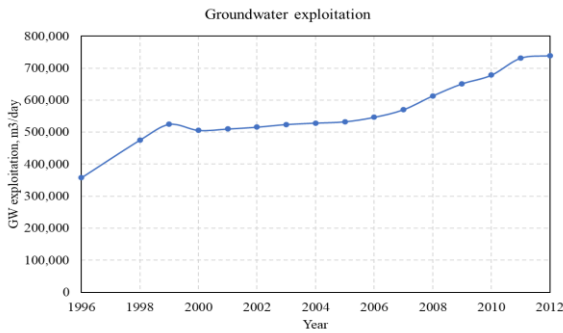


Fig. 1 Groundwater exploitation in Ho Chi Minh City, Viet Nam period 1996-2012

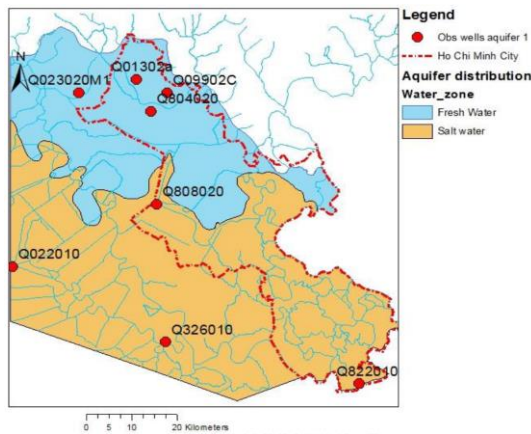


Fig. 2 Upper Pleistocene aquifer distribution map (Khai 2014)

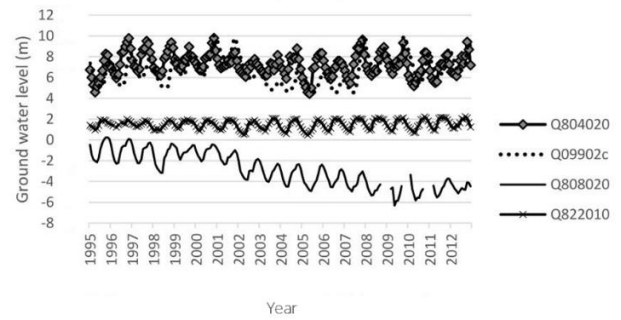


Fig. 3 Groundwater level during 1995-2012 in aquifer 1 at monitoring wells (Khai 2014)

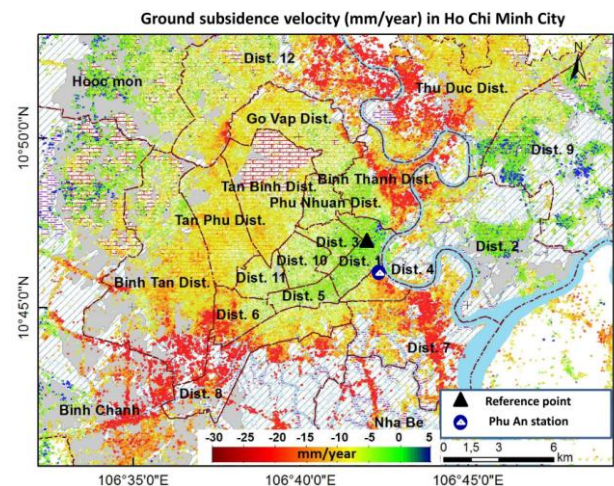


Fig. 4 Average subsidence velocity trend in Ho Chi Minh City from 2006 to 2010 (Minh *et al.* 2015)

2. Groundwater level and ground subsidence in Ho Chi Minh City, Viet Nam

2.1 GWL in Ho Chi Minh City

According to Khai (2014), the aquifers are described by local hydrogeologists as: the upper Pleistocene aquifer, upper-middle Pleistocene aquifer, lower Pleistocene aquifer, middle Pliocene aquifer, and lower Pliocene aquifer. Most (99.7%) of the groundwater used in Ho Chi Minh is supplied from the upper Pleistocene, upper-middle Pleistocene, and lower Pleistocene aquifers (Thoang and Giao 2015). Groundwater exploitation from 1996 to 2012 is shown in Fig. 1 (Khai 2014).

In the current research, the groundwater level was observed from the upper Pleistocene (aquifer 1). The aquifer distribution is shown in Fig. 2. Fig. 3 shows the GWL change in this aquifer from 1995 to 2012. In the city center, the Q822010 well, with rate reduction of GWL equal to 0.33 m/year, is representative of groundwater exploitation. Although the GWL is affected by climate and surface water, reservoir, and seawater levels, the rate of GWL change in the current research was assumed to be constant at 0.33m/year.

2.2 Ground subsidence due to groundwater level change in Ho Chi Minh City, Viet Nam

Ho Chi Minh City is the economic center of Viet Nam with high-speed development. In this condition, the city faces many matters in which the groundwater exploitation for urban and industrial development makes the ground subsidence is the biggest problem in the city.

The ground subsidence in Ho Chi Minh City, Viet Nam has been found since the early years of the 20th century with the development of industrialization and urbanization. The most of reason is groundwater extraction. The average ground subsidence rate was -8 mm/year from 2006 to 2010 (Minh *et al.* 2015). The velocity of ground subsidence is shown in Fig. 4.

Thoang and Giao (2015) indicated that ground subsidence occurred readily due to groundwater pumping. They predicted ground subsidence in Binh Tan district of around 0.44 m after 20 years, a rate of 4.4 cm/year, along the MRT where their research was carried out.

3. FEM modeling using PLAXIS 3D

3.1 Soil and foundation structural modeling

The SGR project located in the Thu Thiem Urban area, a new urban area in Ho Chi Minh City, Viet Nam, was built on Ho Chi Minh subsoil in 2019. It has a height of 73.7 m and consists of 18 stories and one basement floor. The

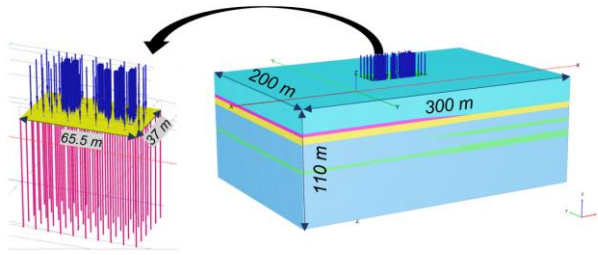


Fig. 5 Typical 3D modeling in PLAXIS 3D

Table 1 Structure parameters

Structure	Raft	Piles
Material Model	Linear elastic	Linear elastic
Thickness t (m)	1.22	-
Diameter D (m)	-	1.2
Unit Weight (kN/m^3)	25	25
Modulus E (kN/m^2)	$3.2e7$	$3.2e7$
Poisson's ratio	0.15	0.15
T_{max} Top (kN/m)	-	70
T_{max} Bot (kN/m)	-	600
F_{max} (kN)	-	8260

building's foundation was laid on a thick layer of very-soft-to-soft clay of Ho Chi Minh subsoil, at 22 – 25 m below the ground surface. Therefore, a piled foundation was chosen for foundation design of this building. The 90 bored piles each had a diameter of 1.2 m and a length of 64.4 m.

PLAXIS 3D, a commercial finite-element package, was used in the current research. The three-dimensional models were simulated by length, width and height of 300 x 200 x 110 and the boundaries of model was fixed in bottom to avoid movement in all directions and sides to avoid movement in lateral directions. Besides, the ground surfaces were free to move all directions. The typical 3D model implementation in this investigation is shown in Fig. 5.

The raft was simulated using a plate element. In PLAXIS 3D, the equivalent value for raft thickness was 1.22 m. The embedded beam is a beam element that interacts with the soil at the pile skin and the pile foot as described by the embedded interface element. In this study, the embedded beam was used to model the bored piles. A linear elastic perfectly plastic interface element was described for the interaction of the pile with the soil. Furthermore, the raft and pile materials were considered as linear elastic with a rigid connection. The input parameters of these structures are shown in Table 1.

The Hardening soil model (HS), which is an advanced model for simulating complex soil, was used to simulate the subsoil of Ho Chi Minh City, Viet Nam. In this model, the strength and Young's modulus are variable with deformations in the consolidation, which was suitable in this research. The input parameters required are plastic straining due to primary deviatoric loading (E_{50}^{ref}), plastic straining due to primary compression (E_{ocd}^{ref}), and elastic

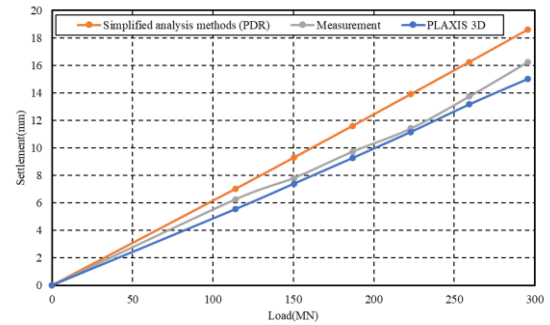


Fig. 6 Comparison between monitoring, PDR method and PLAXIS 3D simulation

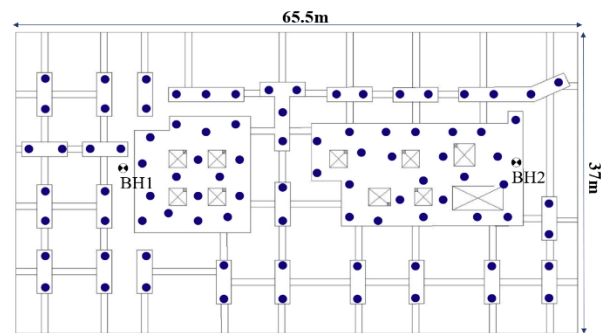


Fig.7 Pile location of actual design

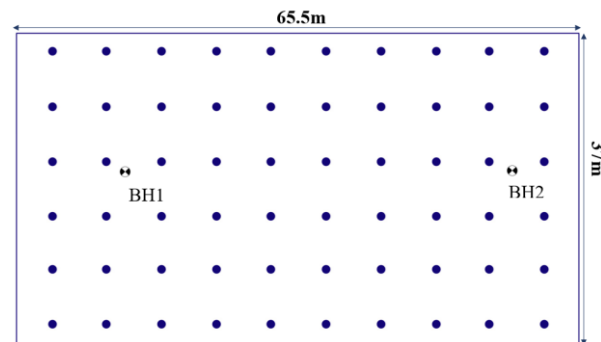


Fig. 8 Pile location of proposed optimal case

unloading-reloading (E_{ur}^{ref}). PLAXIS 3D can simulate multiple boreholes with different soil profiles. The complex soil parameters, used for input into the PLAXIS 3D software, are shown in Table 2. The soil from the ground surface to 20 m depth has an E_{ur}^{ref} value equal to 5 times E_{50}^{ref} (Ngo-Duc 2019). There are 5 kinds of soil that can be modelled: organic clay, dark grey, very-soft-to-soft (1), silty clay, medium-stiff (2a), silty clay, stiff-to-very-stiff (2b), fine to coarse sand, medium-to-very dense (3), and sandy clay and silty clay, stiff-to-very stiff (L3).

To validate the simulation, this PLAXIS 3D model was used to calculate the settlement during the construction period of the project and the results were in good agreement with the monitored settlement in the field and PDR method (Amornfa *et al.* 2022, Quang *et al.* 2021) as shown in Fig. 6. The comparison showed that the numerical simulation via PLAXIS 3D produced relatively good results. Therefore, this model was considered suitable for this research.

Table 2 Soil parameters of BH1 and BH2

Type			Layer 1	Layer 2	Layer 3	Layer 4	Layer 5	Layer 6	Layer 7	Layer 8
			1	2a	2b	3	L3	3	L3	3
Soil type			OH	CH	CH	SM	CL	SM	CL	SM
Materials Model	Unit		HS	HS	HS	HS	HS	HS	HS	HS
Thickness	BH1	m	0-22	22-25.5	25.5-32	32-41	-	41-56	56-59	59-80.5
	BH2	m	0-25	-	25-31	31-41	41-45	45-54	54-61	61-80.5
Unit weight	γ_{sat}	kN/m ³	14.34	14.34	18.5	19.6	19	19.6	19	19.6
	γ_{unsat}	kN/m ³	14.34	14.34	18.5	19.6	19	19.6	19	19.6
Cohesion (c)		kN/m ²	8.9	8.9	28.9	14	32.6	14	32.6	32.6
Friction angle (ϕ)		°	19.9	19.9	23.6	37.7	24.5	37.7	24.5	24.5
Permeability (K)		m/day	6.69E-05	1.68E-05	1.02E-05	8.64E-02	4.42E-06	8.64E-02	4.42E-06	8.64E-02
E ₅₀		kN/m ²	3200	4800	33000	70000	70000	70000	70000	70000
E _{oed}		kN/m ²	1600	2500	33000	70000	70000	70000	70000	70000
E _{ur}		kN/m ²	16000	24000	99000	210000	210000	210000	210000	210000
Poisson's Ratio(v)		-	0.2	0.2	0.2	0.2	0.2	0.2	0.2	0.2
	p _{ref}		100	100	100	100	100	100	100	100
	Power		1	0.9	1	0.5	0.5	0.5	0.5	0.5

Table 3 GWL reduce by global pumping

Period after construction	Current	1 month	6 months	1 year	3 years	5 years	10 years	20 years	50 years
Depth of GWL(m)	-1.1	-1.15	-1.3	-1.43	-2	-2.75	-4.4	-7.7	-17.6

Table 4 GWL in dewatering condition

Change of GWL in dewatering condition	Current	5 m	10 m	15 m	20 m
Depth of GWL(m)	-1.1	-6.1	-11.1	-16.1	-21.1

According to Amornfa *et al.* (2022), pile spacing equal of 5.5D - 6D was proposed as the optimal design, in which the number of piles was reduced compared with the actual design pile spacing of 4.3D, with the settlement increasing, but not by much. Consequently, a case pile spacing of 6D and a reduction of the pile number from 90 to 60 piles was considered as the proposed optimal case in this study, as shown in Figs. 7 and 8.

3.2 GWL change in PLAXIS 3D software

In this research, the first case involved a GWL reduction with time using global groundwater pumping. It was assumed to be linear, based on the Q822010 well in Khai (2014), with a reduced velocity of 0.33 m/year. Table 3 shows the GWL reductions due to global groundwater pumping for PLAXIS 3D. The consolidation and the GWL reduction were combined in PLAXIS 3D to simulate the situation of the GWL reduction due to global groundwater pumping in the field.

The second case is dewatering, which considered the GWL reduction without time. In this case, every point below the structure's foundation and the soil around the project was assumed to be subjected to the same effect when dewatering occurred. The GWL reduction in PLAXIS

3D, as shown in Table 4, was applied to simulate the dewatering in the field without consolidation.

Based on the Terzaghi *et al.* (1996), the effective vertical stress can be calculated

$$\sigma' = \sigma_v - u \quad (1)$$

$$u = \gamma_w \cdot H_w \quad (2)$$

Thus, the GWL reduced as H_w reduced. According to Eqs. (1) and (2) the GWL reduction cause the effective vertical stress increase.

PLAXIS 3D is based on Terzaghi *et al.* (1996). In addition, the pore pressure in PLAXIS 3D is divided into two parts: steady - state pore pressure (P_{steady}) and excess pore pressure (P_{excess}), as shown in Eq. (3) (BV 2020)

$$\sigma = \sigma' + m(p_{steady} + p_{excess}) \quad (3)$$

Where m is a vector containing unity terms for the normal stress components and zero terms for the shear stress components. P_{steady} is the steady-state pore pressure generated in the input program based on the GWL. It is determined before the calculation starts. P_{excess} is the excess pore water pressure during the consolidation process in PLAXIS 3D.

When the load is applied to the soil, the total stress divides into pore pressure and effective stress, as shown in Eq. (3). When the GWL suddenly decreases in PLAXIS 3D, decreases in P_{steady} are equal to increases in P_{excess} . Those are the pore pressure condition in concept of groundwater reduction. Additionally, the pore pressure decreases during the consolidation time, where P_{excess} decreases and

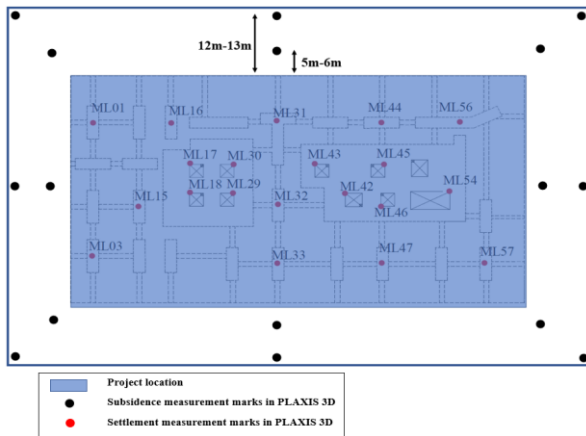


Fig.9 Subsidence measurement locations

settlement occurs. This represents the conditions for pore pressure that are applied in consolidation in PLAXIS 3D.

3.3 Total settlement of foundation and subsidence measurement in PLAXIS 3D

The total settlement of the foundation is the maximum settlement, which measured at the raft depth (-7.2 m below the surface) below the highest column load.

There are 16 locations shown in Fig. 9 that were plotted in PLAXIS 3D to measure the ground surface settlement. The marks are identified with 2 circles. The borderline distance to the first and second circles was 5 – 6 m and 12 – 13 m, respectively. The average settlement value was considered as the subsidence of the ground surface.

4. Results

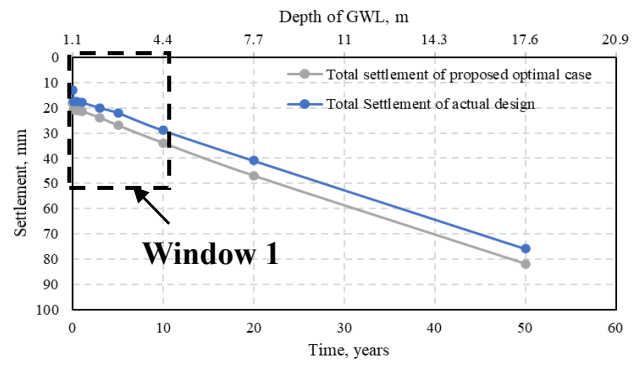
4.1 GWL change due to the global groundwater pumping

The effect of GWL change due to the global groundwater pumping was studied for consolidation times of 1 month, 6 months, 1 year, 3 years, 5 years, 10 years, 20 years, and 50 years with the resultant GWL values being -1.1, -1.15, -1.3, -1.43, -2, -2.75, -4.4, -7.7, and -17.6 m below the ground surface, respectively. The calculations were done for the actual design and the proposed optimal design cases based on Quang *et al.* (2021) and Amornfa *et al.* (2022).

Fig. 10 shows the settlement of the foundation of the actual design when the GWL was reduced due to global groundwater pumping. The total settlement increased when the GWL reduced and was 13 mm immediately after construction and 76 mm 50 years after construction.

In the proposed optimal case, the GWL reduction caused the total increased settlement of the foundation structure of 18 mm immediately after construction to 27 mm after 5 years and 82 mm after 50 (Fig. 10), which agreed with Beygi *et al.* (2019) of GWL reduce by global groundwater pumping and dewatering.

Comparison of the settlement between the foundation



Window 1

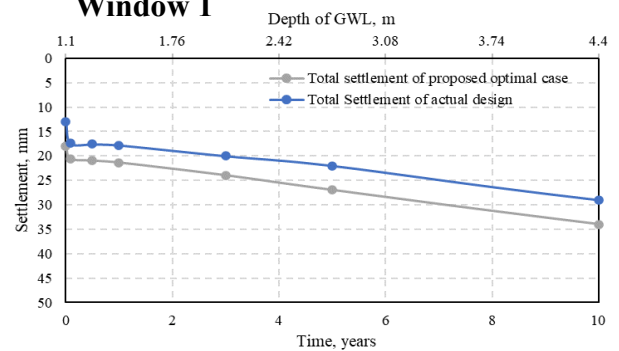
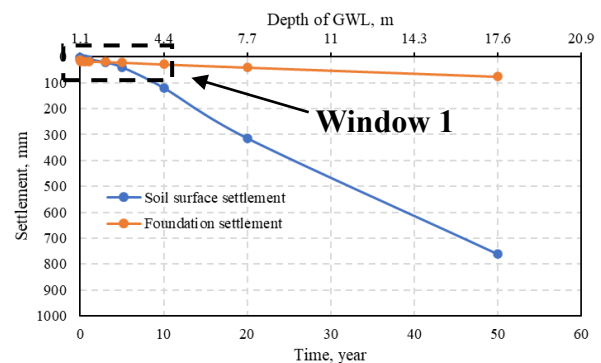


Fig. 10 Total settlement for actual design case and proposed optimal case



Window 1

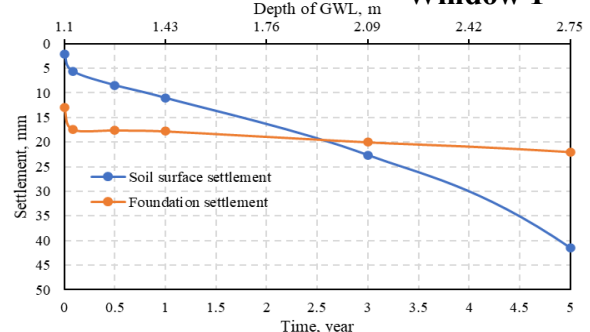


Fig. 11 Comparison of settlement between foundation and soil surface for actual design case

structure and the soil surface for the actual design case is shown in Fig. 11. The contour settlement 1 year and 5 years after construction of the foundation and soil surface

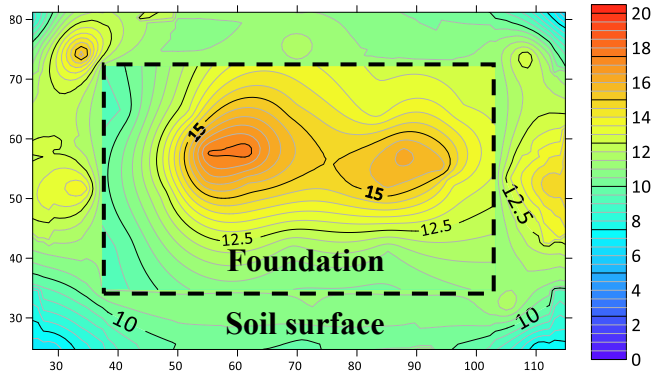


Fig. 12 Settlement contours of the foundation and soil surface after 1 year for actual design

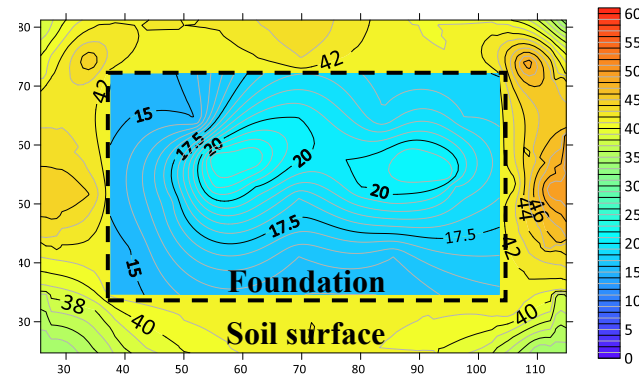


Fig. 13 Settlement contours of the foundation and soil surface after 5 years for actual design

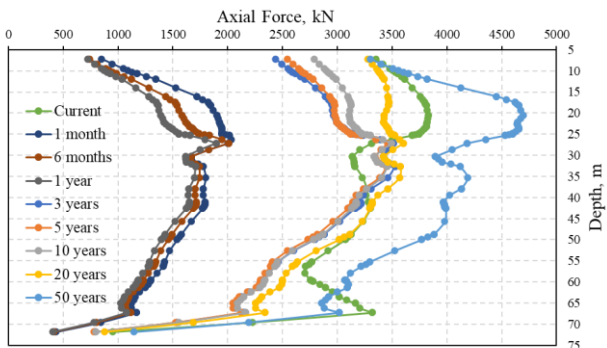


Fig. 14 Axial force of center pile for actual design case

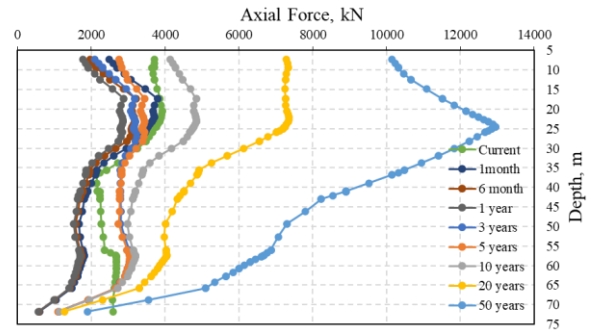


Fig. 15 Axial force of corner pile for actual design case

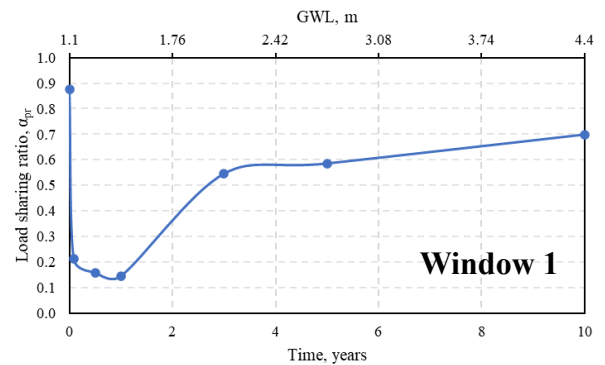
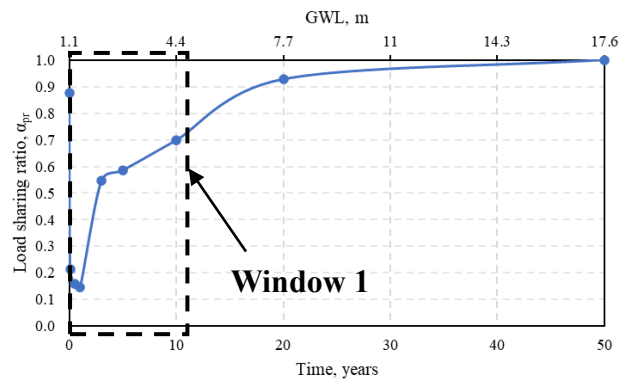


Fig. 16 Load sharing ratio of piles in actual design case

illustrate the representative change of settlement in Figs. 12 and 13, respectively.

From immediately after construction to around 2.5 years after construction, the foundation settlement was higher than the soil surface settlement. In this period, the load from pile transfer to soil was positive during the consolidation time. Therefore, the axial force in a pile reduced, as shown in Figs. 14 and 15.

In the period 2.5 years after construction, the soil surface settlement increased greatly and was higher than the foundation settlement. At that time, the subsidence of the soil affected the foundation. The load transfer from pile to soil was negative (negative skin friction); in other words, the axial force in a pile increased, as shown in Figs. 14 and 15.

The load sharing ratio (α_{pr}), which was affected by the GWL change, was determined based on (Reul and Randolph 2003), as shown in Eq. (4)

$$\alpha_{pr} = \frac{\sum P_{pile}}{P_{tot}} \quad (4)$$

where $\sum P_{pile}$ and P_{tot} are the total load carried by piles and the total applied load, respectively.

Value for α_{pr} in the actual design case are shown in Fig. 16. It can be clearly seen that α_{pr} reduced in the period to 2.5 years after construction, where the soil surface settlement was lower than the foundation settlement. From 2.5 years to 50 years after construction, α_{pr} increased to 1 at 50 years after construction.

Fig. 17 shows the soil surface settlement compared with the foundation settlement of the proposed optimal case. From immediately post construction to 3.4 years, the soil

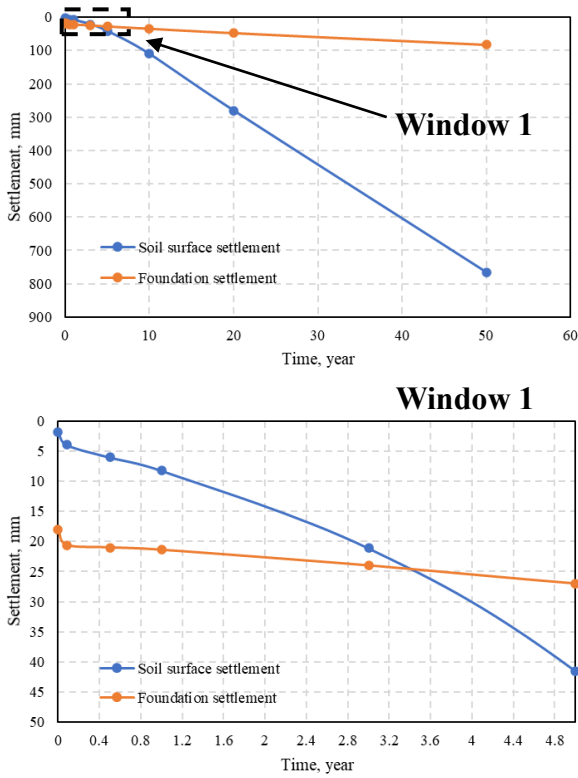


Fig. 17 Comparison of settlement between foundation and soil surface for proposed optimal case

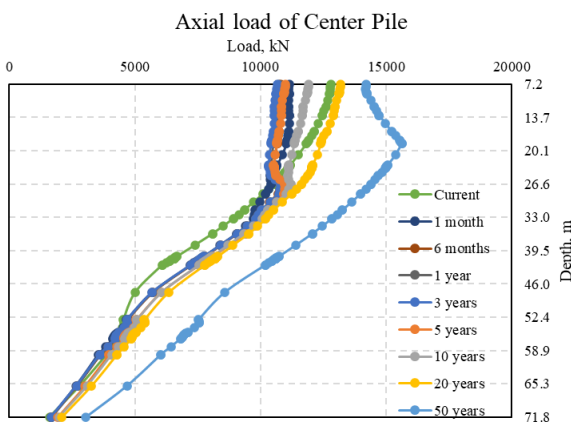


Fig. 18 Axial force of center pile for proposed optimal case

surface settlement was smaller than the settlement of the structure because load transfer from the pile to the soil was positive during this period of consolidation. Thus, the axial force in the piles decreased for this condition. At 3.4 years after construction, the soil surface settlement was higher than the foundation settlement, indicating the negative load transfer (negative skin friction), which was the reason for the increased axial force in the piles as shown in Figs. 18 and 19. Changes in the settlement contours between the foundation and soil surface are shown clearly in Figs. 20 and 21.

Fig. 22 shows α_{pr} values for the proposed optimal case. From immediately post construction to 3 years after construction, α_{pr} reduced from 0.8 to 0.5, due to the positive

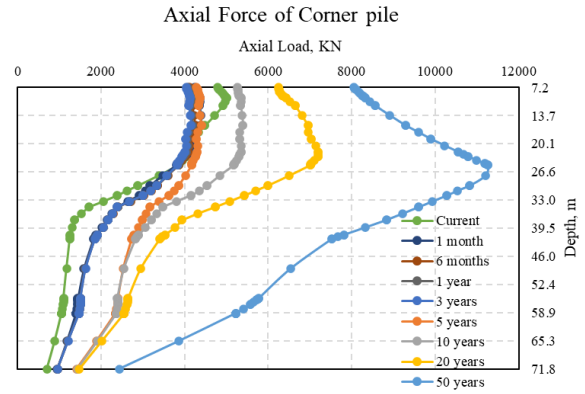


Fig. 19 Axial force of corner pile for proposed optimal case

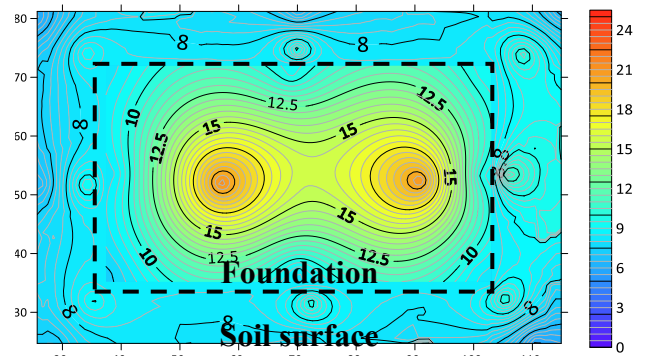


Fig. 20 Settlement contours of foundation and soil surface after 1 year for proposed optimal case

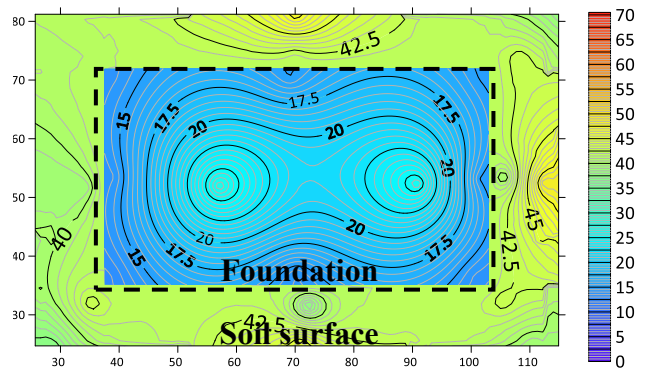


Fig. 21 Settlement contours of foundation and soil surface after 5 years for proposed optimal case

transfer of the load from the pile to the surrounding soil. At 3 years after construction, α_{pr} increased due to the subsidence from 0.5 to 1 at 50 years after construction.

4.2 GWL change due to the dewatering

The effect of GWL change due to dewatering on the piled raft foundation was modelled in PLAXIS 3D using values of 5 m, 10 m, 15 m, and 20 m, for depth resulting on GWL values of -6.1 m, -11.1 m, -16.1 m, and -21.1 m, respectively. This was based on the actual design and proposed optimal case from Quang *et al.* (2021) and Amornfa *et al.* (2022).

The foundation settlement increased a little when the

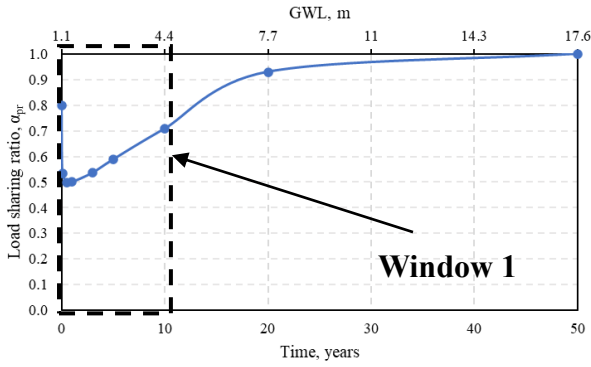


Fig. 22 Load sharing ratio of piles for proposed optimal case

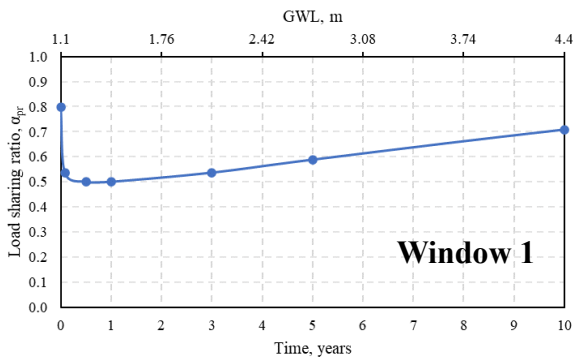


Fig. 23 Total settlement for actual design case and proposed optimal case

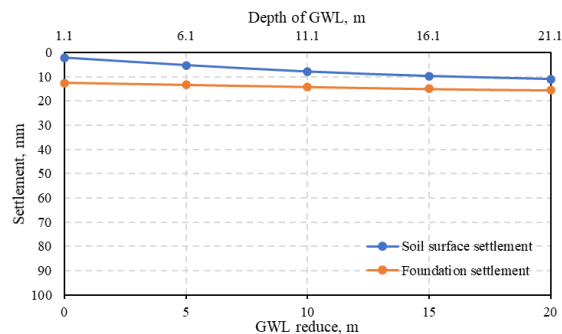


Fig. 24 Comparison of settlement between soil surface and foundation for actual design case

GWL was reduced by dewatering (12.6 mm at construction and 15.5 mm when the GWL was reduced to 20 m immediately), as shown in Fig. 23.

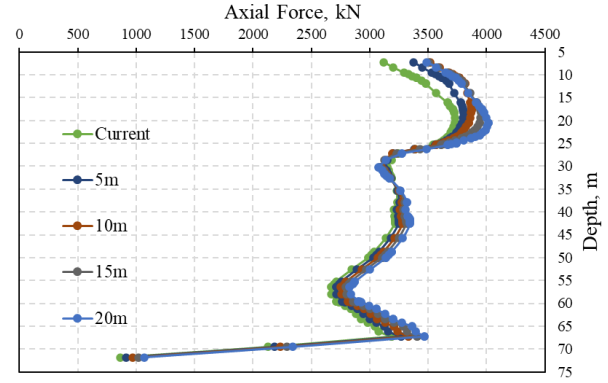


Fig. 25 Axial force of center pile in the actual design

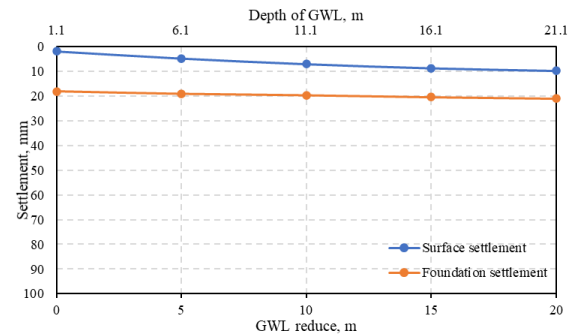


Fig. 26 Comparison of settlement between soil surface and foundation for proposed optimal case

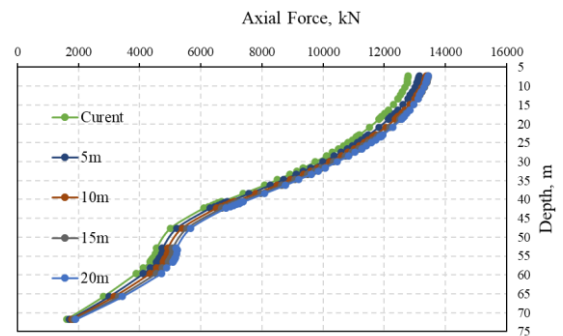


Fig. 27 Axial force of center pile for proposed optimal case

Fig. 24 provides a settlement comparison between the foundation and the soil surface. It can be clearly seen that the settlement of the foundation was greater than for the soil surface. Therefore, there was a positive transfer of load from the pile to the soil in a short time. Thus, the axial force in the pile rose only a little, making it negligible in the dewatering conditions, as illustrated in Fig. 25.

For the proposed optimal case, as the GWL decreased, there was a small increase in settlement, being almost linear in each 5 m GWL reduction (18 mm at construction and 21 mm in GWL reduced to 21.1m from the ground surface quickly), as shown in Fig. 23.

The ground surface settlement was small and less than the foundation settlement, but only for a brief period when dewatering occurred, as shown in Fig. 26. Consequently, the axial force in the pile increased, but only slightly, as shown in Fig. 27.

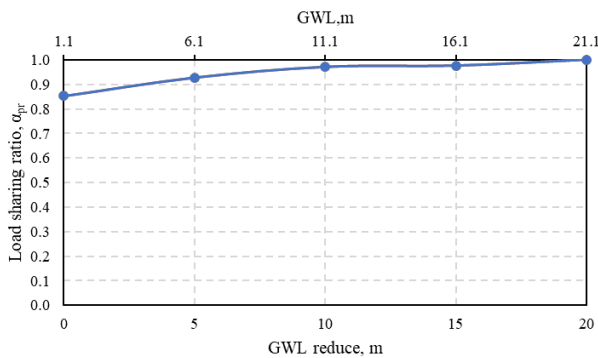


Fig. 28 Load sharing ratio for actual design case

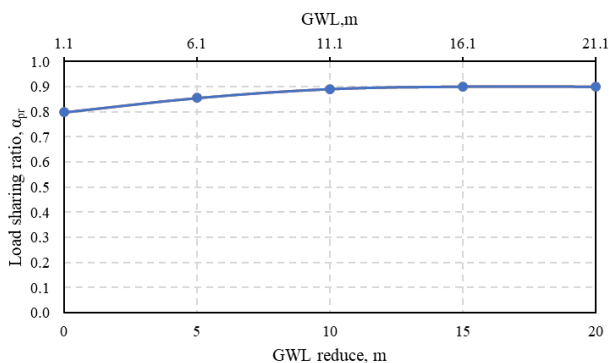


Fig. 29 Load sharing ratio for proposed optimal case

As the axial force in the piles increased, the α_{pr} values for the actual design and the proposed optimal case increased, as the GWL was reduced by dewatering. Figs. 28 and 29 show those increments, with $\alpha_{pr} = 1$ in the actual design case as the GWL was reduced to 21.1 m. In the proposed optimal case, α_{pr} increased from 0.8 to 0.9 as the GWL was reduced from current value to 21.1m. It can be clearly seen α_{pr} for the actual design was higher than for the proposed optimal case from the GWL in the current until it was reduced to 21.1 m by the dewatering method.

5. Conclusions

3D-FEM analysis was used to investigate the settlement behavior and axial force of a pile raft as affected by GWL conditions. The GWL change due to global groundwater pumping and dewatering in Ho Chi Minh subsoil was modelled in the PLAXIS 3D analysis. The main conclusions were that the settlement of the foundation increased more when the GWL lowered over time, which were found for both actual design and proposed optimal case (pile spacing equal to 6D). The negative transfer of load from the pile to the soil (negative skin friction), occurred due to the subsidence. The effect of ground subsidence was evident 2.5 years after construction for the actual design and 3.4 years after construction for the proposed optimal case. The axial force along the piles increased during this period. The load sharing ratio was affected for both the actual design and proposed optimal

case and decreased in the period before ground subsidence and then increased when the ground subsidence occurred. The ground subsidence occurred due to the GWL change that affected the foundation, in particular, and the infrastructure in general. Furthermore, there are many issues that will affect the construction industry if GWL pumping cannot be controlled in the near future, due to rapid urbanization, industrialization, and population growth. Charging and other policies for groundwater exploitation are necessary to underpin successful ongoing development in Ho Chi Minh City, Viet Nam.

PLAXIS 3D was used to simulated dewatering using GWL reduction. The total settlement of the structure's foundations increased a little as the GWL lowered during in dewatering conditions for both the actual design case and the proposed optimal case. The axial force increased, but it was too small to have a pronounced effect. Due to dewatering, the increases in pile axial force were not substantially affected by GWL change. However, α_{pr} increased when the GWL was reduced by the dewatering. The load was almost entered by piles in case the GWL was reduced to 21.1 m below the ground surface.

Acknowledgements

This research was partially supported by a grant from the Faculty of Engineering at Kamphaeng Saen, Kasetsart University, Thailand. A Graduate Program Scholarship was provided by the Department of Civil Engineering, Faculty of Engineering at Kamphaeng Saen, Kasetsart University, Thailand.

References

- Amornfa, K., Pheinwej, N. and Kijpayuck, P. (2012), "Current practice on foundation design of high-rise buildings in Bangkok, Thailand", *Lowland Technol. Int.*, **14**, 70-83.
- Amornfa, K., Quang, H.T. and Tuan, T.V. (2022), "3D numerical analysis of piled raft foundation for Ho Chi Minh City subsoil conditions", *Geomech. Eng.*, **29**(2), 183-192. <https://doi.org/10.12989/gae.2022.29.2.183>.
- Bandyopadhyay, S., Sengupta, A. and Parulekar, Y.M. (2020), "Behavior of a combined piled raft foundation in a multi-layered soil subjected to vertical loading", *Geomech. Eng.*, **21**(4), 379-390. <https://doi.org/10.12989/gae.2020.21.4.379>.
- Bernardes, H.C., Carvalho, S.L., Sales, M.M., Almeida, S.R.M.D., Farias, M.M.D. and Pinho, F.A.X.C. (2019), "Hybrid numerical tool for nonlinear analysis of piled rafts", *Soils Found.*, **59**(6), 1659-1674. <https://doi.org/10.1016/j.sandf.2019.04.011>.
- Beygi, M., Keshavarz, A., Abbaspour, M. and Vali, R. (2019), "3D numerical study of the piled raft behaviour due to groundwater level changes in the frictional soil", *Int. J. Geotech. Eng.*, **14**(6), 665-672. <https://doi.org/10.1080/19386362.2019.1677326>.
- BV, P. (2020). *Scientific*, Plaxis 3D Manual. Plaxis bv, Bentley Systems, Incorporated, Netherlands.
- Fattah, M.Y., Al-Mosawi, M.J. and Al-Zayadi, A.A.O. (2013), "Time dependent behavior of piled raft foundation in clayey soil", *Geomech. Eng.*, **5**(1), 17-36. <https://doi.org/10.12989/gae.2013.5.1.017>.
- Gu, L.L., Ye, G.L., Bao, X.H. and Zhang, F. (2016), "Mechanical behaviour of piled-raft foundations subjected to high-speed train

- loading”, *Soils Found.*, **56**(6), 1035-1054. <https://doi.org/10.1016/j.sandf.2016.11.008>.
- Hoang, L.T. and Matsumoto, T. (2020), “Long-term behavior of piled raft foundation models supported by jacked-in piles on saturated clay”, *Soils Found.*, **60**(1), 198-217. <https://doi.org/10.1016/j.sandf.2020.02.005>.
- Huang, M., Jiu, Y., Jiang, J. and Li, B. (2017), “Nonlinear analysis of flexible piled raft foundations subjected to vertical loads in layered soils”, *Soils Found.*, **57**(4), 632-644. <https://doi.org/10.1016/j.sandf.2017.04.004>.
- Katzenbach, R., Arslan, U. and Moormann, C. (2000), *Piled Raft Foundation Projects in Germany*, 323-391. J.A. Hemsley, Design Applications of Raft Foundations. ICE Publishing.
- Khai, H.Q. (2014), “Impact of climate change on groundwater recharge in Ho Chi Minh City area”. Master Thesis, Chulalongkorn University.
- Khanmohammadi, M. and Fakharian, K. (2018), “Evaluation of performance of piled-raft foundations on soft clay: A case study”, *Geomech. Eng.*, **14**(1), 43-50. <https://doi.org/10.12989/gae.2018.14.1.043>.
- Kitiyodom, P., Matsumoto, T. and Sonoda, R. (2011), “Approximate numerical analysis of a large piled raft foundation”, *Soils Found.*, **51**, 1-10. <https://doi.org/10.3208/sandf.51.1>.
- Ko, J., Cho, J. and Jeong, S. (2018), “Analysis of load sharing characteristics for a piled raft foundation”, *Geomech. Eng.*, **16**(4), 449-461. <https://doi.org/10.12989/gae.2018.16.4.449>.
- Minh, D.H.T., Trung, L.V. and Toan, T.L. (2015), “Mapping ground subsidence phenomena in Ho Chi Minh City through the radar interferometry technique using alos palsar data”, *Remote Sens.*, **7**(7), 8543-8562. <https://doi.org/10.3390/rs70708543>.
- Nakanishi, K. and Takewaki, I. (2013), “Optimum pile arrangement in piled raft foundation by using simplified settlement analysis and adaptive step-length algorithm”, *Geomech. Eng.*, **5**(6), 519-540. <https://doi.org/10.12989/gae.2013.5.6.519>.
- Ngo-Duc, T. (2019), “Determination of the Unloading - Reloading Modulus and Exponent Parameters (M) for Hardening Soil Model from Drained Triaxial Test of Soft Soil in Ho Chi Minh City”, *Modern Environ. Sci. Eng.*, **5**, 207-216. [https://doi.org/10.15341/mesc\(2333-2581\)/01.05.2019/001](https://doi.org/10.15341/mesc(2333-2581)/01.05.2019/001).
- Poulos, H.G. (2012), “Foundation design for tall buildings”, *Geotechnical Engineering State of the Art and Practice*.
- Quang, H.T., Amornfa, K. and Tuan, T.V. (2021), “Piled raft - an effective foundation design method for high-rise buildings in Ho Chi Minh City, Viet Nam”, *Int. J. Geomate*, **21**(87), 102-109. <https://doi.org/10.21660/2021.87.j2341>.
- Reul, O. and Randolph, M.F. (2003), “Piled rafts in overconsolidated clay-comparison of in situ measurements and numerical analysis”, *Géotechnique*, **53**(3), 301-315. <https://doi.org/10.1680/geot.2003.53.3.301>.
- Roh, Y., Kim, I., Kim, G. and Lee, J. (2019), “Comparative analysis of axial load capacity for piled-raft foundation with changes in groundwater level”, *KSCCE J. Civil Eng.*, **23**(10), 4250-4258. <https://doi.org/10.1007/s12205-019-0239-3>.
- Sawada, K. and Takemura, J. (2014), “Centrifuge model tests on piled raft foundation in sand subjected to lateral and moment loads”, *Soils Found.*, **54**(2), 126-140. <https://doi.org/10.1016/j.sandf.2014.02.005>.
- Tan, Y.C., Cheah, S.W. and Tahal, M.R. (2006), *Methodology for Design of Piled Raft for Five-Storey Buildings on Very Soft Clay*, 226-233. Foundation Analysis and Design: Innovative Methods. Geotech. Spec. Publ. (ASCE).
- Terzaghi, K., Peck, R.B. and Mesri, G. (1996), *Soil Mechanics in Engineering Practice*, John Wiley & Sons, Inc, Canada.
- Thoang, T.T. and Giao, P.H. (2015), “Subsurface characterization and prediction of land subsidence for Hcm City, Vietnam”, *Eng. Geol.*, **199**, 107-124. <https://doi.org/10.1016/j.enggeo.2015.10.009>.
- Tran, T.V., Kimura, M. and Boonyatee, T. (2012), “3D FE analysis of effect of ground subsidence and piled spacing on ultimate bearing capacity of piled raft and axial force of piles in piled raft”, *Open J. Civil Eng.*, **2**(4), 206-213. <https://doi.org/10.4236/ojce.2012.24027>.
- Vali, R. and Foroughi Boroujeni, F. (2022), “Ground surface displacements and failure mechanisms induced by Epb shield tunneling method and groundwater levels changes”, *Transport. Infrastruct. Geotech.*, <https://doi.org/10.1007/s40515-022-00239-1>.
- Vali, R., Mehrinejad Khotbehsara, E., Saberian, M., Li, J., Mehrinejad, M. and Jahandari, S. (2017), “A three-dimensional numerical comparison of bearing capacity and settlement of tapered and under-reamed piles”, *Int. J. Geotech. Eng.*, **13**(3), 236-248. <https://doi.org/10.1080/19386362.2017.1336586>.
- Vo, P.L. (2008), “Urbanization and water management in Ho Chi Minh City, Vietnam-issues, challenges and perspectives”, *Geo J.*, **70**(1), 75-89. <https://doi.org/10.1007/s10708-008-9115-2>.
- Watcharasawe, K., Jongpradist, P., Kitiyodom, P. and Matsumoto, T. (2021), “Measurements and analysis of load sharing between piles and raft in a pile foundation in clay”, *Geomech. Eng.*, **24**(6), 559-572. <https://doi.org/10.12989/gae.2021.24.6.559>.
- Yamashita, K., Tanikawa, T. and Hamada, J. (2015), “Applicability of simple method to piled raft analysis in comparison with field measurements”, *Geotech. Eng. J. SEAGS & AGSSEA*, **46**(2), 43-52.
- Yamashita, K., Yamada, T. and Hamada, J. (2011), “Investigation of settlement and load sharing on piled rafts by monitoring full-scale structures”, *Soils Found.*, **51**(3), 513-532. <https://doi.org/10.3208/sandf.51.513>.

IC